

# Long-term serial non-invasive multislice computed tomography angiography with functional evaluation after coronary implantation of a bioresorbable everolimus-eluting scaffold: the ABSORB cohort B MSCT substudy

Yoshinobu Onuma<sup>1,2†</sup>, Carlos Collet<sup>3†</sup>, Robert-Jan van Geuns<sup>1</sup>, Bernard de Bruyne<sup>4</sup>, Evald Christiansen<sup>5</sup>, Jacques Koolen<sup>6</sup>, Pieter Smits<sup>7</sup>, Bernard Chevalier<sup>8</sup>, Dougal McClean<sup>9</sup>, Dariusz Dudek<sup>10</sup>, Stephan Windecker<sup>11</sup>, Ian Meredith<sup>12</sup>, Koen Nieman<sup>1,2</sup>, Susan Veldhof<sup>13</sup>, John Ormiston<sup>14</sup>, and Patrick W. Serruys<sup>15\*</sup>; on behalf of the ABSORB Investigators

<sup>1</sup>Department of Interventional Cardiology, ThoraxCenter, Erasmus University Medical Center, s-Gravendijkwal 230, 3015 CE Rotterdam, The Netherlands; <sup>2</sup>Cardiology Department, Academic Medical Center, Meibergdreef 9, 1105 AZ Amsterdam-Zuidoost, Amsterdam, The Netherlands; <sup>3</sup>Cardiology Department, Academic Medical Center, Amsterdam, Cardialysis, Westblaak 98, 3012 KM Rotterdam, The Netherlands; <sup>4</sup>Department of Cardiology, Onze-Lieve-Vrouwziekenhuis, Moorselbaan 164, 9300 Aalst, Belgium; <sup>5</sup>Department of Cardiology, Skejby Sygehus, Aarhus Universitet Skejby Sygehus, Brendstrupgårdsvej 100, 8200 Aarhus N, Denmark; <sup>6</sup>Department of Cardiology, Catharina Ziekenhuis, Michelangelolaan 2, 5623 EJ Eindhoven, the Netherlands; <sup>7</sup>Department of Cardiology, Maasstad Ziekenhuis, Maasstadweg 21, 3079 DZ, Rotterdam, the Netherlands; <sup>8</sup>Department of Interventional Cardiology, Institut Hospital Jacques Cartier, 6 Avenue du Noyer Lambert, 91300 Massy, France; <sup>9</sup>Department of Cardiology, Christchurch Hospital, 2 Riccarton Ave, Christchurch Central, Christchurch 4710, New Zealand; <sup>10</sup>Jagiellonian University Institute of Cardiology, University Hospital Krakow, Mikołaja Kopernika 36, 31-501 Kraków, Poland; <sup>11</sup>Universitätsklinik für Kardiologie, Inselspital, Freiburgstrasse 4, 3010 Bern, Switzerland; <sup>12</sup>Monash Heart, Monash Medical Centre, 246 Clayton Rd, Clayton VIC 3168, Melbourne, Australia; <sup>13</sup>Clinical Development, Abbott Vascular, Diegem, Belgium; <sup>14</sup>Department of Cardiology, Auckland City Hospital, 2 Park Rd, Grafton, Auckland 1023, New Zealand; and <sup>15</sup>Imperial College London Kensington, London SW7 2AZ, UK

Received 27 October 2016; editorial decision 30 January 2017; accepted 1 February 2017; online publish-ahead-of-print 16 March 2017

## Aims

Multimodality invasive imaging of the first-in-man cohort demonstrated at 5 years stable lumen dimensions and a low rate of major adverse cardiac events (MACE). However, the long-term non-invasive assessment of this device remains to be documented. The objective was to describe the 72-month multislice computed tomography (MSCT) angiographic and functional findings after the implantation of the second iteration of the fully resorbable everolimus-eluting polymeric scaffold.

## Methods and results

In the ABSORB Cohort B trial patients with non-complex *de novo* lesions were treated with second iteration bioresorbable vascular scaffold (BVS). MSCT angiography was performed as an optional investigation at 18 months; patients were re-consented for a second investigation at 72 months. MSCT data were analysed at independent core laboratories for quantitative analysis of lumen dimensions and for calculation of fractional flow reserve derived from computed tomography (FFR<sub>CT</sub>). From the overall Cohort B (101 patients), 53 patients underwent MSCT imaging at 72 months. The MACE rate was 1.9% (1/53). At 72 months, the median minimal lumen area (MLA) was 4.05 mm<sup>2</sup> (interquartile range [IQR]: 3.15–4.90) and the mean percentage area stenosis was 18% (IQR: 4.75–31.25), one scaffold was totally occluded. In 39 patients with paired MSCT analysis, the MLA significantly increased from the first to the second follow-up ( $\Delta = 0.80$  mm<sup>2</sup>,  $P = 0.002$ ). The change in the median FFR<sub>CT</sub> scaffold gradient between time points was zero.

\* Corresponding author. Tel: +31 102062828; Fax: +31 107044759. E-mail: patrick.w.j.c.serruys@pwserruys.com

† These authors contributed equally to this work.

Published on behalf of the European Society of Cardiology. All rights reserved. © The Author 2017. For permissions, please email: journals.permissions@oup.com.

**Conclusion** The long-term serial non-invasive MSCT evaluation with  $\text{FFR}_{\text{CT}}$  assessment after bioresorbable scaffold implantation confirmed in-scaffold late lumen enlargement with the persistence of normalization of the  $\text{FFR}_{\text{CT}}$ .

**Clinical trial registration** URL: <http://www.clinicaltrials.gov>. Unique identifier: NCT00856856.

**Keywords** scaffold • coronary computed tomography angiography • fractional flow reserve derived from computed tomography

## Introduction

Despite the inherent risk of caging the coronary artery with metallic stent, percutaneous coronary interventions (PCI) have been demonstrated to be of clinical benefit in patients with ischaemic coronary artery disease.<sup>1</sup> However, the concept of a fully resorbable technology has attracted the interventional community since the early days of PCI. The bioresorbable vascular scaffolds have been developed and introduced into clinical practice.<sup>2</sup> The temporal scaffolding of the coronary artery has the advantage of preventing acute vessel closure after balloon dilatation, delivering anti-restenotic drugs to the vessel wall to control the process of restenosis while restoring the natural integrity of the vessel.<sup>3</sup> Moreover the polymeric backbone of the scaffold is radio-lucent and does not interfere with the assessment of the opacified lumen using non-invasive multislice computed tomography (MSCT) angiography, providing an alternative to invasive angiography for the follow-up of the patients treated with PCI.

The second iteration of the fully resorbable everolimus-eluting scaffold was tested in the ABSORB (ABSORB Clinical Investigation, Cohort B Everolimus Eluting Coronary Stent System Clinical Investigation) trial. (Study Sponsor Abbott Vascular). Patients with non-complex *de novo* coronary artery lesion were included and studied with multimodality imaging at short, mid, and long-term after implantation (i.e., from 6 months to 60 months). Invasive findings with angiography, intravascular ultrasound (IVUS), virtual histology (VH) and optical coherence tomography (OCT) showed that bioresorption of polymeric struts occurs at 3 years and is associated with late lumen enlargement, plaque, and media reduction, restoration of vasomotion and cyclic strain.<sup>4</sup> In addition, mid-term MSCT evaluation (i.e. 18 months) was shown to be feasible with a scaffold patency observed in 91% of the cases ( $n = 67$ ); however, long-term non-invasive MSCT follow-up remains to be documented.

Computed tomography technology has vastly improved over the past decades. The spatial resolution achieved by the latest generation CT scanners has been shown to provide an accurate assessment of the coronary artery lumen. Furthermore, physiological parameters such as fractional flow reserve derived from computed tomography ( $\text{FFR}_{\text{CT}}$ ) can also be computed using computational fluid dynamics in a 3-D coronary model thereby providing additional information to the purely anatomical evaluation.<sup>5</sup>

We sought to evaluate the angiographic and functional outcomes after the treatment of obstructive coronary artery disease with the second iteration of the bioresorbable polymeric everolimus-eluting scaffold by means of serial (18 and 72 months) non-invasive MSCT coronary angiographic plus functional  $\text{FFR}_{\text{CT}}$  assessment.

## Methods

### Study design

The design of this study has been previously reported.<sup>6</sup> Briefly, this was a single-arm, prospective, open-label, efficacy, and safety study. One hundred and one patients were enrolled at 12 centres between March and November 2009. The overall cohort (B) was subdivided into two groups of patients: the first group (B1) underwent invasive imaging with quantitative coronary angiography, IVUS grayscale, VH and OCT at 6, 24, and 60 months, whereas the second group (B2) underwent invasive imaging at 12, 36, and 60 months; both groups underwent non-invasive cardiac MSCT angiography at 18 months. Before the end of the 5-year follow-up, the protocol was amended to allow the patients who had undergone a MSCT scan as an optional investigation at 18 months to be re-consented to undergo a second MSCT scan at 72 months. From the overall cohort of 101 patients, 80 patients were eligible for re-consent (reasons for not being approached for re-consent ( $n = 21$ ) are shown in Supplementary data online, *Table S1* appendix). Fifty-three patients were consented, 23 refused, 4 could not be reached.

### Study device and procedure

The bioresorbable vascular scaffold (BVS) 1.1 balloon-expandable device consists of a polymer backbone of poly-L-lactide (PLLA) coated with a thin layer of a 1:1 mixture of poly(L-lactide-co-D,L-lactide) (PDLLA) polymer and the antiproliferative drug everolimus containing 100  $\mu\text{g}$  everolimus/ $\text{cm}^2$  scaffold. The implant is radiolucent but has two platinum markers of 244  $\mu\text{m}$  at each end that allows easy visualization on MSCT and other imaging modalities. PDLLA allows controlled release of the everolimus so that 80% has been eluted by 30 days. Both PLLA and PDLLA are fully resorbable.<sup>7</sup> The scaffolding procedure has been previously described. Briefly, target lesions were treated using standard interventional techniques with mandatory predilatation. Bailout stenting with a Xience-V drug-eluting stent for edge dissection and insufficient coverage of the lesion was recommended if needed. Treatment with aspirin was started at least 24 h before the procedure and was followed by life-long aspirin treatment according to guidelines of the European Society of Cardiology/American Heart Association/American College of Cardiology. A loading dose of 300 mg clopidogrel was administered before the procedure, followed by 75 mg daily for a minimum of 6 months.<sup>8,9</sup>

### MSCT angiography

Cardiac MSCT angiography was performed at 18 months and 72 months with the use of a 64-slice computed tomography technology or beyond (Supplementary data online, *Table S2* appendix). Standard acquisition techniques were used, which included the use of nitrates prior to image acquisition and beta-blockers in patients with a fast heart rate ( $> 65$  bpm), tube settings depending on patient body mass index (80–140 kV), and axial scan protocols for patients with lower heart rates to reduce

radiation doses, all at the discretion of the individual sites. Images were reconstructed using thin slices (0.5–0.67 mm) and medium smooth reconstruction filters in different phases. All data were stored on a DVD for core laboratory evaluation.

### MSCT analysis

Data from MSCT was analysed off-line by an independent Corelab (Cardalys BV, Rotterdam, The Netherlands) using a validated cardiovascular analysis package (Circulation, Siemens AG, Forchheim, Germany).<sup>10</sup> Vessel cross-sections were reconstructed at approximately 1 mm longitudinal increments, extending 5 mm beyond the device, using the remaining platinum scaffold indicators as landmarks. Automatic lumen segmentation of the vessel lumen, with manual correction was performed to measure the lumen area. The outer vessel borders were manually traced to approximate the vessel size, using a window display setting: level, 750 Hounsfield units; width, 250 Hounsfield units, the window level was adjusted if necessary. The mean, minimal lumen area (MLA), and maximum lumen areas were determined for each scaffold. The reference lumen area was calculated as the average between the mean vessel area proximal and distal to the scaffolded segments. The luminal percentage area stenosis was calculated as the difference between the MLA and the reference as a percentage of the reference. A significant area of stenosis was defined as  $\geq 75\%$ , which approximates 50% diameter stenosis. Mean plaque burden (PB) in the scaffolded region was defined as mean vessel area minus mean lumen area divided by mean vessel area. Plaque composition was qualitatively assessed for the presence of non-calcified plaque, calcified plaque and mixed plaque at each cross-section.<sup>11–13</sup> The percentage of cross sections of each plaque type was calculated as a number of cross sections with the plaque type divided by the total number of cross sections analysed in the scaffolded segment.

### FFR<sub>CT</sub> analysis

The FFR<sub>CT</sub> was performed by an independent core laboratory at HeartFlow, Inc. (Redwood City, California, USA). The detailed methodology is described elsewhere.<sup>14</sup> Using the most recent generation of FFR<sub>CT</sub> analysis software, for each patient a quantitative 3-D anatomic model of the aortic root and epicardial coronary arteries was generated from coronary MSCT images for each patient.<sup>15</sup> Since the new software iteration enables more accurate FFR<sub>CT</sub> analysis and higher acceptance rate, the 18-month data was re-analysed by this software. In addition, any patient with a paired MSCT investigation that was analysed originally at 18 months was re-analysed using the new version of the FFR<sub>CT</sub> software. Coronary blood flow and pressure were computed under conditions simulating maximal hyperaemia. Blood was assumed to be a Newtonian fluid. The FFR<sub>CT</sub> results are presented as FFR<sub>CT</sub> distal to the scaffold and FFR<sub>CT</sub> gradient, defined as the difference between the FFR<sub>CT</sub> distal and proximal to the scaffold.

### Definitions

The composite clinical endpoint is cardiac death, MI classified as Q-wave and non-Q-wave MI, and ischaemia-driven (ID) target lesion revascularization (TLR). ID TLR implies revascularization at the target lesion, irrespective of the time window for angiographic control at 6 months or 2 years, associated with: (i) a positive functional ischaemia study; (ii) ischaemic symptoms and angiographic minimal lumen diameter stenosis  $\geq 50\%$  by core laboratory quantitative coronary angiography (QCA); or (iii) revascularization of a target lesion with a diameter stenosis  $\geq 70\%$  by core laboratory QCA without either ischaemic symptoms or a positive functional study. For a diagnosis of non-Q wave MI, elevation of creatine kinase levels two times the upper limit of normal with increased creatine kinase myocardial band was required. Scaffold thrombosis was

adjudicated according to the Academic Research Consortium definitions. Other clinical endpoints include all-cause mortality, non-ID TLR, and ID or non-ID target vessel revascularization (TVR).<sup>16</sup>

### Statistical analysis

Binary variables are presented as percentages and continuous variables as mean and standard deviation or median and interquartile range (IQR), depending on the distribution. Serial (i.e. 18 and 72 months) paired analysis is presented in tables. For the paired comparisons the Wilcoxon signed rank test was used. For the computation of luminal area and percentage area stenosis, total occlusions (TO) were computed with a MLA of 0 mm<sup>2</sup> and area stenosis 100%, whereas cases with TO were excluded for the paired analysis. All statistical analyses were performed with SPSS software version 23.0 (IBM Corporation, Armonk, New York).

## Results

### Baseline characteristics and clinical follow-up

Overall, 101 patients were included in this study. Baseline demographics and five years clinical outcomes have been previously published (Table 1).<sup>4</sup> For the cohort of 53 patients who underwent MSCT imaging at 72 months, the major adverse cardiac events rate at 5 years was 1.9% (1/53), with a TVF (Cardiac Death, MI, ID-TLR, ID-TVR) rate of 3.8% (2/53). This was attributable to one in-hospital MI and one ID Non-TLR TVR between the second and third year. There were no changes in event rates between the fifth and sixth year.

In 11 centres, 72 patients underwent MSCT angiography at 18 months, and at a median of 6.1 years (IQR 6.02–6.23) a second MSCT angiography was performed in 53 patients. At 6 years, quantitative MSCT angiographic analysis was feasible in 46 (87%) cases. No quantitative analysis was possible in three patients due to poor MSCT quality; however, in these cases visual percentage area stenosis  $\leq 50\%$  was found (Figure 1). One patient had an in-scaffold total occlusion not related to an event. The median minimal luminal area was 4.05 mm<sup>2</sup> (IQR: 3.15–4.90) and the mean percentage area stenosis was 18% (IQR: 4.75–31.25) (Figure 2).

### Anatomical changes assess by mulstislice CT angiography

Vascular changes were assessed in 39 paired patients by means of serial MSCT angiography (i.e. 18 months and 72 months; Table 2). The in-scaffold MLA significantly increased from the first to the second follow-up ( $\Delta = 0.80$  mm<sup>2</sup>,  $P = 0.002$ ). This was associated with a significant reduction in PB ( $\Delta = -3.9\%$ ,  $p = 0.004$ ) and a non-significant reduction in plaque area ( $\Delta = -0.27$  mm<sup>2</sup>,  $P = 0.451$ ) and in vessel area ( $\Delta = 0.16$ ,  $P = 0.717$ ). Figure 3 depicts the cumulative frequency curve of the lumen, plaque and vessel area. Plaque composition in the scaffolded region changed significantly. The number of cross-sections with non-calcified plaque was reduced by 19.3% ( $P = 0.001$ ) whereas the number of cross-sections with mixed plaque increased by 20.1%. At the proximal edge, a significant increase in the median minimal luminal area was also observed (from 3.70 mm<sup>2</sup> [IQR: 3.00–4.85 mm<sup>2</sup>] at 18 months to 4.45 mm<sup>2</sup> [IQR 3.50–5.18 mm<sup>2</sup>] at 72 months,  $P = 0.025$ ). At the distal edge, no significant changes in lumen, plaque or vessel areas were found.

**Table 1** Baseline characteristics

	Overall (n = 101)	MSCT 6-year Cohort (n = 53)	No MSCT (n = 48)	P-value
Age (mean ± SD), years	62.2 ± 8.9	61.2 ± 8.9	63.4 ± 8.8	0.228
Male sex, n (%)	73 (72)	38 (72)	35 (73)	0.891
Diabetes mellitus, n (%)	17 (17)	7 (13)	10 (21)	0.306
Current smoker n (%)	17 (17)	11 (21)	6 (13)	0.288
Hyperlipidaemia requiring medication, n (%)	79 (78)	39 (74)	40 (83)	0.236
Hypertension, n (%)	62 (62)	34 (65)	28 (58)	0.486
Prior CABG, n (%)	3 (3)	1 (2)	2 (4)	0.500
Prior myocardial infarction, n (%)	25 (25)	12 (23)	13 (27)	0.644
Treated vessel				0.732
Left anterior descending, n (%)	44 (43)	21 (39.6)	22 (45.8)	
Left circumflex, n (%)	24 (24)	13 (24.5)	10 (20.8)	
Right coronary artery, n (%)	34 (34)	18 (34)	16 (33.3)	
AHA/ACC lesion classification				0.476
A, n (%)	1 (1)	1 (1.9)	1 (2.1)	
B1, n (%)	55 (55)	32 (60.4)	23 (47.9)	
B2, n (%)	40 (40)	17 (32.1)	23 (47.9)	
C, n (%)	4 (4)	2 (3.8)	2 (4.2)	
Mean reference vessel diameter, mm	2.61 ± 0.37	2.57 ± 0.37	2.53 ± 0.65	0.682
Minimum luminal diameter, mm	1.06 ± 0.28	1.05 ± 0.24	1.01 ± 0.37	0.556
Diameter stenosis, %	59 ± 10	58.67 ± 9.31	57.04 ± 16.13	0.536
Lesion length, mm	9.9 ± 3.6	9.66 ± 3.49	9.78 ± 4.32	0.706

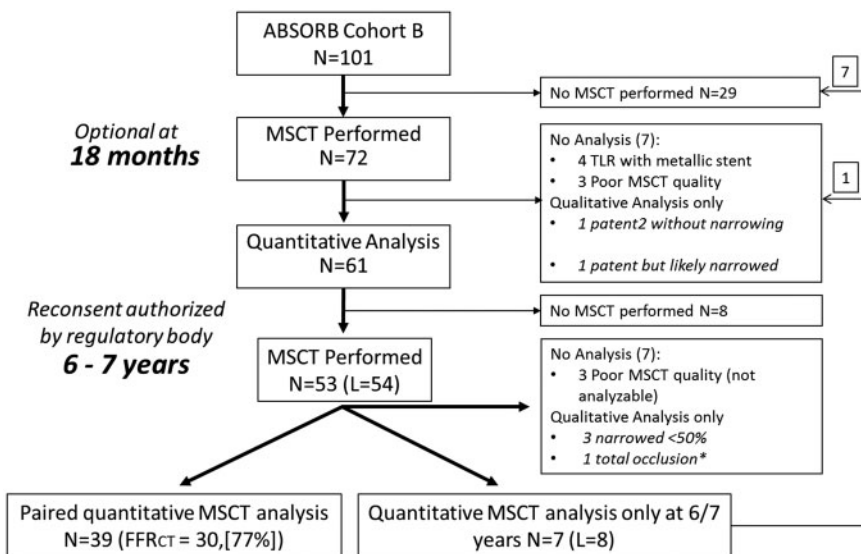


**Figure 1** Patient flowchart of 72-month follow-up. After 72-month follow-up, 53 patients were re-consented for long-term MSCT angiography evaluation. Quantitative analysis was possible 46 patients (47 scaffolds). \* In one patient a total occlusion in-scaffold was found. MSCT, Multislice computed tomography; TLR, Target lesion revascularization; FFRCT, Non-invasive fractional flow reserve derive from multislice computed tomography.

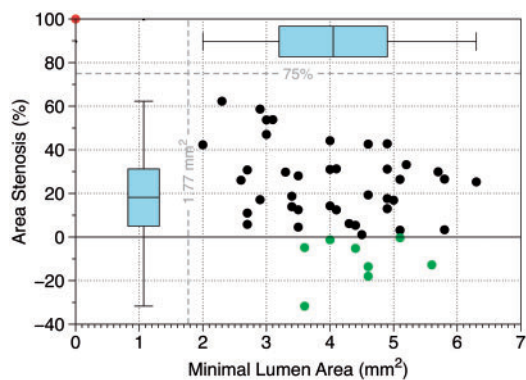


**Figure 2** Minimal lumen area versus Percentage Area Stenosis in the Scaffold Segment at 72 months ( $n = 48$ ). The median of MLA and area stenosis was  $4.05 \text{ mm}^2$  (IQR:  $3.15\text{--}4.90$ ) and  $18.18\%$  (IQR:  $4.75\text{--}31.25$ ), respectively. The dashed lines indicate 75% area stenosis (or 50% diameter stenosis) and  $1.77 \text{ mm}^2$  is 25% of nominal area of scaffold of  $3.0 \text{ mm}$  (e.g.  $7.07 \text{ mm}^2$ ). The patient with in-scaffold total occlusion is depicted with the red dot and patients with negative percentage area stenosis in green dots.

## Serial non-invasive fractional flow reserve

Of the 39 patients with paired MSCT analysis,  $\text{FFR}_{\text{CT}}$  computations were feasible in 30 (77%) patients. In nine cases,  $\text{FFR}_{\text{CT}}$  analysis was not possible due to large slice thickness or pixel spacing ( $n = 4$ ), clipped myocardium ( $n = 2$ ), motion artefact ( $n = 1$ ), missing data in the CT image ( $n = 1$ ) and previous coronary artery bypass graft surgery ( $n = 1$ ). At 72 months, the  $\text{FFR}_{\text{CT}}$  distal to the scaffold was  $0.88$  (IQR:  $0.82\text{--}0.92$ ) which was similar to the distal  $\text{FFR}_{\text{CT}}$  found at 18 months ( $\Delta = 0.02$ ,  $P = 0.367$ ). There were two asymptomatic patients with  $\text{FFR}_{\text{CT}} < 0.80$  with a minimum lumen area  $< 4.00 \text{ mm}^2$  treated medically and one symptomatic patient in whom an  $\text{FFR}_{\text{CT}}$  of  $0.79$  with a MLA of  $2.3 \text{ mm}^2$  was found; this patient underwent a diagnostic cardiac catheterization and found a severe lesion distal to the scaffold with a positive invasive FFR, and consequently underwent ID-non-TLR-TV-PCI. The scaffold gradient at 72 months was  $-0.035$  (IQR:  $-0.053$  to  $-0.010$ ) with a delta scaffold gradient of  $0$  ( $-0.013\text{--}0.010$ ) between time points (Figure 4). Figure 5 shows the changes of MLA,  $\text{FFR}_{\text{CT}}$  distal to the scaffold and  $\text{FFR}_{\text{CT}}$  scaffold gradient at 18 and 72 months.

## Discussion

The present analysis represents the longest non-invasive imaging follow-up of patients treated with the Bioresorbable Everolimus-

**Table 2** Serial Quantitative MSCT Assessment at 18 and 72 months

	18 months	72 months	Difference (72–18 months)	P-value
<b>In-Scaffold, <math>\text{mm}^2</math> (<math>n = 39</math>)</b>				
Minimal Lumen Area	3.20 (2.80 to 4.20)	4.00 (3.10 to 4.90)	0.60 (-1.0 to -0.20)	0.002
Mean lumen area	4.94 (3.83 to 6.30)	5.76 (4.41 to 6.45)	-0.51 (0.13 to 0.92)	0.019
Mean vessel area	13.64 (10.53 to 16.79)	12.96 (11.00 to 15.87)	0.16 (-1.06 to 0.84)	0.717
Mean plaque area	8.57 (6.32 to 10.92)	8.06 (5.68 to 9.72)	-0.27 (-0.44 to 1.16)	0.451
Mean reference area	4.22 (3.50 to 5.60)	4.68 (3.9 to 6.01)	0.52 (-1.05 to -0.075)	0.026
Plaque Burden (%)	62.8 (58.7 to 67)	59 (53.5 to 64.5)	-3.93 (-6.31 to -1.52)	0.004
Area stenosis, %	23.2 (11.42 to 32.55)	16.9 (3.33 to 29.91)	-4.3 (-5.35 to 12.67)	0.357
Cross sections with noncalcified plaque, %	81.8 (41.18 to 100.0)	62.5 (35.71 to 80.00)	-10.6 (4.36 to 16.97)	0.001
Cross sections with mixed plaque, %	17.4 (0 to 56.67)	37.5 (20.00 to 64.29)	11.4 (-17.59 to -5.29)	0.001
Cross sections with calcified plaque, %	0 (0 to 0)	0 (0 to 0)	0 (0 to 0)	0.109
<b>Proximal segment, <math>\text{mm}^2</math> (<math>n = 36</math>)</b>				
Minimal Lumen Area	3.70 (3.00 to 4.85)	4.45 (3.50 to 5.18)	0.65 (-1.15 to -0.15)	0.025
Mean lumen area	4.53 (3.64 to 5.87)	5.17 (4.05 to 5.87)	0.51 (-0.96 to 0.30)	0.065
Mean vessel area	12.40 (9.20 to 15.0)	13.10 (9.40 to 16.30)	1.00 (-2.20 to 0.30)	0.106
Mean plaque area	7.0 (5.11 to 8.99)	7.49 (4.74 to 10.08)	0.49 (-1.33 to 0.62)	0.315
<b>Distal segment, <math>\text{mm}^2</math> (<math>n = 36</math>)</b>				
Minimal Lumen Area	3.60 (2.83 to 4.58)	3.75 (3.03 to 4.70)	0.35 (-0.80 to 0.15)	0.192
Mean lumen area	4.07 (3.33 to 5.43)	4.46 (3.49 to 5.67)	0.47 (-0.98 to 0.30)	0.072
Mean vessel area	10.80 (8.0 to 14.05)	11.10 (7.63 to 14.50)	0.35 (-1.55 to 1.13)	0.590
Mean plaque area	6.31 (4.46 to 8.43)	5.72 (4.09 to 7.91)	0.19 (-0.86 to 1.27)	0.683
<b><math>\text{FFR}_{\text{CT}}</math> (<math>n = 30</math>)</b>				
Proximal to Scaffold	0.91 (0.85 to 0.95)	0.93 (0.87 to 0.96)	0.01 (-0.03 to 0.005)	0.236
Distal to Scaffold	0.89 (0.82 to 0.92)	0.88 (0.82 to 0.92)	0.005 (-0.030 to 0.020)	0.626
Scaffold Gradient	-0.030 (-0.048 to -0.020)	-0.035 (-0.050 to -0.013)	0 (-0.010 to 0.010)	0.896
Delta (72–18 months) Gradient		0 (-0.018 to 0.010)		



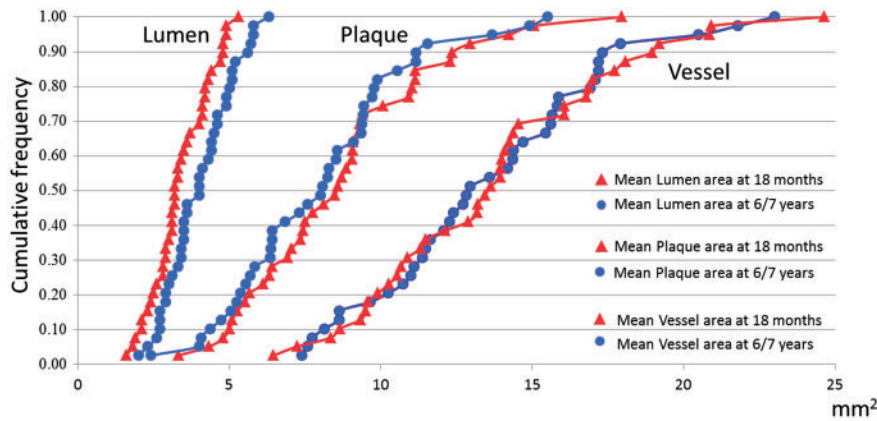


**Figure 3** Cumulative Frequency Distribution Curves of Mean Lumen Area, Plaque Area, and Vessel Area at 18 and 72 months ( $n = 39$ ). All frequency distribution as assessed by multislice computed tomography.

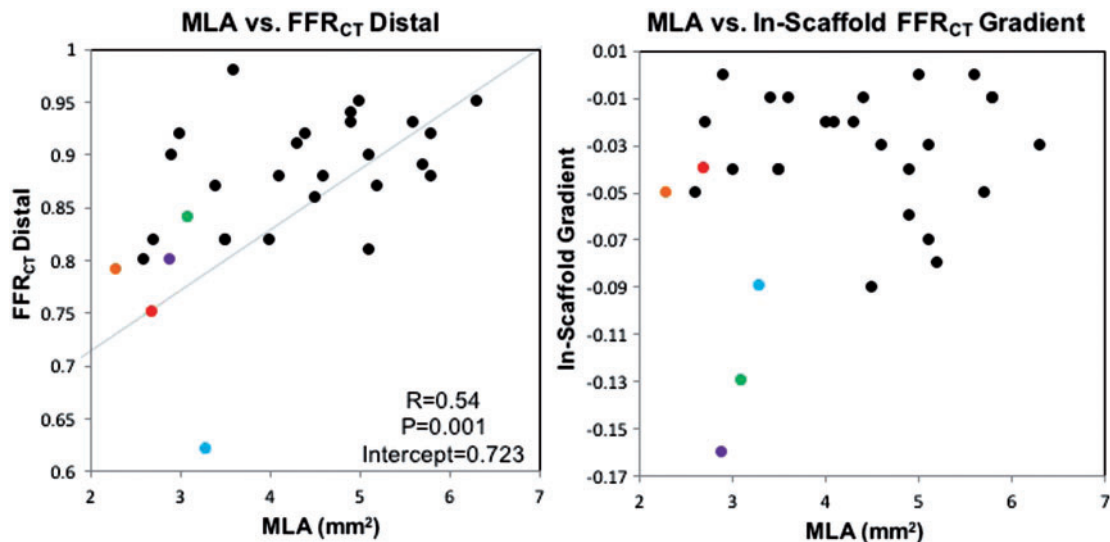


**Figure 4** Minimum lumen area versus non-invasive FFR at 72 months ( $n = 30$ ). (Left) A scatter plot of non-invasive FFR<sub>CT</sub> distal to the scaffold versus MLA in-scaffold assessed by multislice computed tomography at 72 months. (Right) A scatterplot of the change in FFR<sub>CT</sub> across the scaffolded segment (scaffold gradient = distal FFR<sub>CT</sub>-proximal FFR<sub>CT</sub>) vs. MLA in-scaffold. There were three patients with FFR<sub>CT</sub> distal to the scaffold < 0.80. In two patients (blue and red dot), the positive FFR<sub>CT</sub> was due to an in-scaffold FFR<sub>CT</sub> deterioration. In one patient (orange dot), a combination of proximal disease progression and in-scaffold deterioration was responsible for the positive FFR<sub>CT</sub> distal to the scaffold. The patient with the greater in-scaffold drop (purple dot), had a decrease of in-scaffold MLA from 4.2–2.9 mm<sup>2</sup>; however, FFR<sub>CT</sub> distal to the scaffold at 72 months remained at 0.80. Depicted with a green dot, a patient with in-scaffold deterioration with a FFR<sub>CT</sub> > 0.80 distal to the scaffold. MLA, Minimal lumen area; FFR<sub>CT</sub>, Non-invasive fractional flow reserve derived from multislice computed tomography; FFR, Fractional Flow Reserve; PCI, Percutaneous coronary intervention.

Eluting Scaffold. In addition, for the first time a serial assessment of the functional component of a treated region is presented. The principal finding of this study is the durability of the initial angiographic

results with a significant late lumen enlargement in the scaffolded region and the persistence of normalization of the FFR<sub>CT</sub> (Figures 6 and 7).

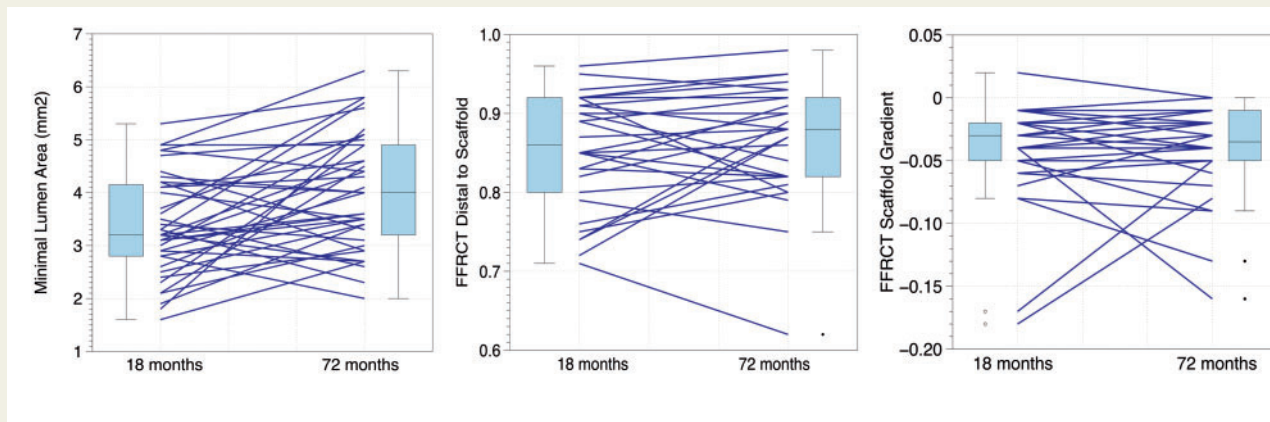


**Figure 5** Delta minimal lumen area, FFR<sub>CT</sub> Distal to the Scaffold and Scaffold Gradient between 18 months and 72 months. (Left) Delta MLA ( $n = 39$ ) showing an overall significant increase in median MLA ( $\Delta = 0.67 \text{ mm}^2$ ,  $P = 0.019$ ). (Middle) Delta distal FFRCT ( $n = 30$ ) depicting a non-significant change ( $\Delta = -0.005$ ,  $P = 0.626$ ) between 18 and 72 months. (Right). Delta gradient reflecting no significant deterioration of FFRCT across the scaffold ( $\Delta = 0$ ,  $P = \text{NS}$ ) between 18 and 72 months.

From 18 to 72 months after implantation a significant increase in the MSCT-derived mean and minimal luminal area was found. Late luminal gain has been observed in long-term follow-up of patients treated with bioresorbable scaffolds. With the first iteration of this device, evaluated in ABSORB Cohort A, after the early decrease in IVUS-derived MLAs, an increase in mean and minimal luminal areas was observed from 6 months to 2 years. This phenomenon was associated with a decrease in plaque area without changes in vessel area. In ABSORB Cohort B, a similar finding of increase in the IVUS-derived mean luminal area with a decrease in plaque area was also demonstrated. The restoration of the natural integrity of the vessel, which responds to pulsatile flow (i.e. mechanotransduction) triggering atheroprotective signals (e.g. eNOS gene regulation, steady-levels of prostacyclin, etc.) in combination with drug elution might contribute to adapt the uncaged vessel to the physiologic stimuli.<sup>17,18</sup> Moreover, late lumen enlargement might have a clinical impact. At the scaffolded region, the enlarged lumen increases blood flow and pressure and influence the haemodynamic microenvironment contributing, in some cases, to the normalization of the FFR<sub>CT</sub> and shear stress. Therefore, scaffolding in combination with optimal medical therapy (i.e. HMG-CoA reductase inhibitors and potentially PCSK9 inhibitors) has the potential to improve the durability of the results after PCI.

The interaction between the scaffold, its degradation process and the progression or regression of atherosclerosis is not yet fully understood.<sup>19</sup> In the present analysis, a non-significant reduction in mean plaque and vessel area was found. Nonetheless, a significant reduction in plaque burden was observed. Moreover, an increase in the calcified component of the plaque behind the scaffold depicted by an increase in the number of cross-sections with mixed plaque (calcified plus non-calcified plaques) and a parallel decrease in non-calcified plaque was found. It can be hypothesized that the presence of the drug-eluting scaffold might play a role in plaque stabilization. However, the increase in the calcified component of the plaque could also be attributed to the natural history of the atherosclerotic process. Recently,

adverse plaque characteristics (i.e. low attenuation plaque, positive remodelling and spotty calcification) have been shown to be associated with ischaemia. However, the interplay between plaque characteristics, endothelial function, and myocardial ischaemia requires further study.<sup>20–22</sup> The strategy of plaque stabilization is currently being tested in the PREVENT (Preventive implantation of bioresorbable vascular scaffold on stenosis functional insignificant with signs of vulnerability) trial and in PROSPECT II & PROSPECT ABSORB (A multicentre prospective natural history study using multimodality imaging in patients with acute coronary syndromes combined with a randomized, controlled, intervention study) trial, which will further increase our knowledge of the impact of fully Bioresorbable Everolimus-Eluting Scaffold as an atherosclerosis stabilization strategy.<sup>23,24</sup>

The feasibility of the non-invasive FFR<sub>CT</sub> with the new software iteration was higher than in previous publications.<sup>7</sup> Furthermore, in six cases which had been previously rejected for FFR<sub>CT</sub> analysis at 18 months, re-assessment with the new software allowed for the computation of FFR<sub>CT</sub>. The software improvements in image segmentation and refinements in the construction of physiological models raised the acceptability of MSCT data for FFR<sub>CT</sub> analysis. In this study, for the first time, a serial FFR<sub>CT</sub> analysis after bioresorbable Everolimus-eluting scaffold implantation is presented. In 30 paired cases, there was no evidence of deterioration of the FFR<sub>CT</sub> between 18 months and 72 months. In addition, to specifically evaluate the device performance, the scaffold gradient was quantified (i.e. FFR<sub>CT</sub> distal—proximal to the scaffold). At 72 months, the scaffold gradient confirmed the persistence of the FFR<sub>CT</sub> normalization in the treated region with a delta scaffold gradient of 0 (IQR -0.018–0.010); 27 of 30 patients exhibited a delta scaffold gradient of  $\leq 0.05$ .

In contrast to metallic stents, which hamper luminal assessment with MSCT due to the blooming effect, MSCT evaluation of the bioresorbable scaffold allows the identification of luminal contours providing a reliable angiographic assessment.<sup>25</sup> Additionally, due to the non-invasive nature of this evaluation, patients are more willing to

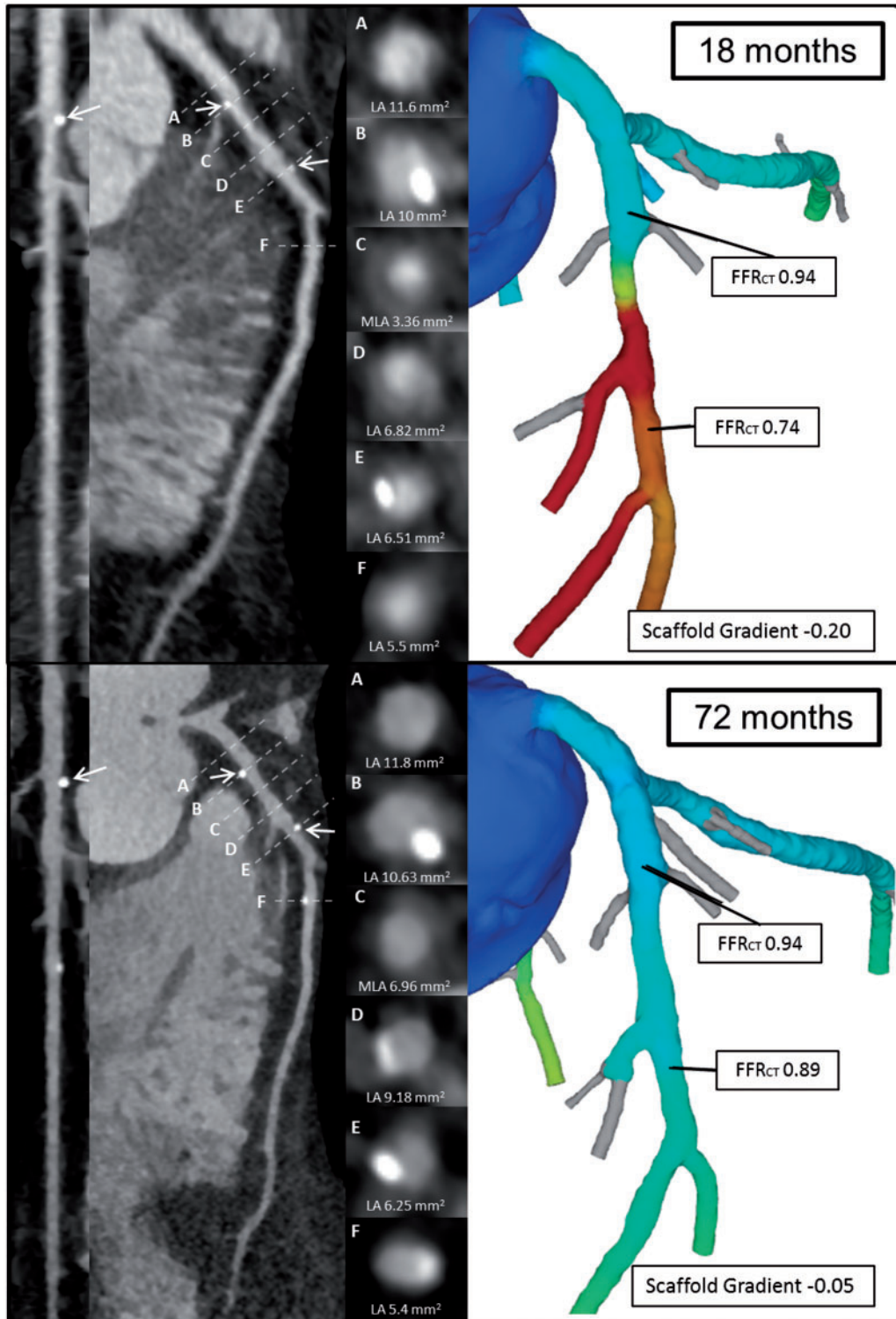


**Figure 6** Case example of serial MSCT with  $FFR_{CT}$  improvement at follow-up. Case example of a patient treated with a Bioresorbable Vascular Scaffold (white arrows) in the proximal segment of the LAD. MSCT angiography at 18 months showed a moderate in-scaffold stenosis with MLA  $3.36 \text{ mm}^2$  (dash line C) with area stenosis of 64%. At 72-month MSCT angiography follow-up, showed an increased MLA to  $6.96 \text{ mm}^2$  (dash line C) and area stenosis of 30%. This late lumen enlargement had a significant impact on  $FFR_{CT}$  distal to the scaffold. Also panel F depict a new calcified plaque in the mid segment of the LAD.  $FFR_{CT}$ , Non-invasive fractional flow reserve derived from multislice computed tomography; LAD, Left anterior descending artery; MLA, Minimal lumen area.



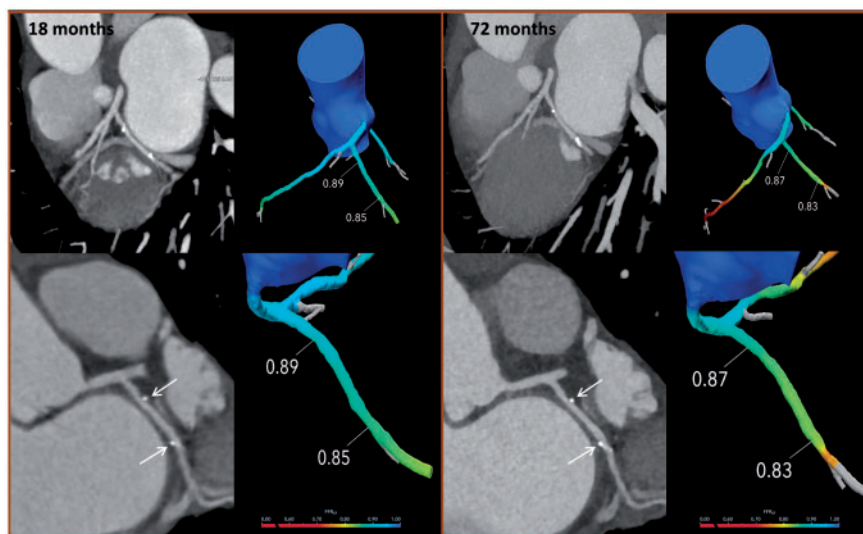


**Figure 7** Case example of serial MSCT with  $FFR_{CT}$  at follow-up. Case example of a patient treated with a Bioresorbable Vascular Scaffold (white arrows) in the proximal segment of the left Circumflex artery. At 18 months (A), MSCT Angiography showed a patent scaffold with MLA of 3.1 mm<sup>2</sup> and  $FFR_{CT}$  scaffold gradient of 4. At 72 months (B), the persistence of the normalization of the  $FFR_{CT}$  in-scaffold with the same gradient was found. However, in the distal edge of the scaffolded region plaque progression with a reduction of the luminal area and  $FFR_{CT}$  was observed.

undergo MSCT compared to standard invasive angiographic evaluation. In the overall ABSORB Cohort B, the attrition rate for invasive imaging follow-up was 50%.<sup>4</sup> For the long-term MSCT evaluation, 70% of the eligible patients were re-consented for a very late follow-up. This might have an implication for the design of future clinical trials with biodegradable scaffolds. Considering the high diagnostic accuracy, the incremental value of the functional evaluation, patient convenience and safety MSCT angiography with  $FFR_{CT}$  offers a reliable alternative to invasive imaging and has the potential to become the method of choice for the follow-up of patients treated with bioresorbable scaffolds.

### Limitations

This first-in-human trial included a non-complex population; therefore, these results should be confirmed in a larger and more complex population. Although the standard MSCT acquisition techniques were used, the scan protocol was adjusted for different CT scanners used at each institution and each follow-up which could have impacted vessel measurements. However, despite these limitations, this study used coronary MSCT in multiple patients and confirmed the occurrence of in-scaffold lumen enlargement. Even though  $FFR_{CT}$  has demonstrated high diagnostic accuracy compared to invasive FFR, discrepancies between the in-scaffold MSCT-derived geometry and the true geometry might have an impact in the  $FFR_{CT}$  results.

### Conclusion

The long-term serial non-invasive MSCT with  $FFR_{CT}$  assessment after bioresorbable scaffold implantation is feasible, with quantitative and

functional diagnosis obtained in the vast majority of patients. The current series confirmed late lumen enlargement and continuance of normalization of the  $FFR_{CT}$ .

### Supplementary data

Supplementary data are available at *European Heart Journal–Cardiovascular Imaging* online.

**Conflicts of interest:** S.V. is an employee of Abbott Vascular. Y.O. and P.W.S. are members of Advisory Board of Abbott Vascular. All other authors declare no competing interests.

### References

- De Bruyne B, Fearon WF, Pijls NH, Barbato E, Tonino P, Piroth Z et al. Fractional flow reserve-guided PCI for stable coronary artery disease. *N Engl J Med* 2014;**371**:1208–17.
- Ormiston JA, Serruys PW, Regar E, Dudek D, Thuesen L, Webster MW et al. A bioabsorbable everolimus-eluting coronary stent system for patients with single de-novo coronary artery lesions (ABSORB): a prospective open-label trial. *Lancet* 2008;**371**:899–907.
- Serruys PW, Ormiston JA, Onuma Y, Regar E, Gonzalo N, Garcia-Garcia HM et al. A bioabsorbable everolimus-eluting coronary stent system (ABSORB): 2-year outcomes and results from multiple imaging methods. *Lancet* 2009;**373**:897–910.
- Serruys PW, Ormiston J, van Geuns RJ, de Bruyne B, Dudek D, Christiansen E et al. A polylactide bioresorbable scaffold eluting everolimus for treatment of coronary stenosis: 5-year follow-up. *J Am Coll Cardiol* 2016;**67**:766–76.
- Onuma Y, Dudek D, Thuesen L, Webster M, Nieman K, Garcia-Garcia HM et al. Five-year clinical and functional multislice computed tomography angiographic results after coronary implantation of the fully resorbable polymeric everolimus-eluting scaffold in patients with *de novo* coronary artery disease: the ABSORB cohort A trial. *JACC Cardiovasc Interv* 2013;**6**:999–1009.
- Ormiston JA, Serruys PW, Onuma Y, van Geuns RJ, de Bruyne B, Dudek D et al. First serial assessment at 6 months and 2 years of the second generation of

- absorb everolimus-eluting bioresorbable vascular scaffold: a multi-imaging modality study. *Circ Cardiovasc Interv* 2012;**5**:620–32.
7. Onuma Y, Serruys PW. Bioresorbable scaffold: the advent of a new era in percutaneous coronary and peripheral revascularization? *Circulation* 2011;**123**:779–97.
  8. Fihn SD, Blankenship JC, Alexander KP, Bittl JA, Byrne JG, Fletcher BJ et al. 2014 ACC/AHA/AATS/PCNA/SCAI/STS focused update of the guideline for the diagnosis and management of patients with stable ischemic heart disease: a report of the American College of Cardiology/American Heart Association Task Force on Practice Guidelines, and the American Association for Thoracic Surgery, Preventive Cardiovascular Nurses Association, Society for Cardiovascular Angiography and Interventions, and Society of Thoracic Surgeons. *J Am Coll Cardiol* 2014;**64**:1929–49.
  9. Windecker S, Kolh P, Alfonso F, Collet JP, Cremer J, Falk V et al. 2014 ESC/EACTS Guidelines on myocardial revascularization: the Task Force on Myocardial Revascularization of the European Society of Cardiology (ESC) and the European Association for Cardio-Thoracic Surgery (EACTS) Developed with the special contribution of the European Association of Percutaneous Cardiovascular Interventions (EAPCI). *Eur Heart J* 2014;**35**:2541–619.
  10. Leber AW, Johnson T, Becker A, von Ziegler F, Tittus J, Nikolaou K et al. Diagnostic accuracy of dual-source multi-slice CT-coronary angiography in patients with an intermediate pretest likelihood for coronary artery disease. *Eur Heart J* 2007;**28**:2354–60.
  11. Voros S, Rinehart S, Qian Z, Joshi P, Vazquez G, Fischer C et al. Coronary atherosclerosis imaging by coronary CT angiography: current status, correlation with intravascular interrogation and meta-analysis. *JACC Cardiovasc Imaging* 2011;**4**:537–48.
  12. Lehman SJ, Schlett CL, Bamberg F, Lee H, Donnelly P, Shturman L et al. Assessment of coronary plaque progression in coronary computed tomography angiography using a semiquantitative score. *JACC Cardiovasc Imaging* 2009;**2**:1262–70.
  13. Leipsic J, Abbara S, Achenbach S, Cury R, Earls JP, Mancini GJ et al. SCCT guidelines for the interpretation and reporting of coronary CT angiography: a report of the Society of Cardiovascular Computed Tomography Guidelines Committee. *J Cardiovasc Comput Tomogr* 2014;**8**:342–58.
  14. Serruys PW, Girasis C, Papadopoulou SL, Onuma Y. Non-invasive fractional flow reserve: scientific basis, methods and perspectives. *EuroIntervention* 2012;**8**:511–9.
  15. Norgaard BL, Leipsic J, Gaur S, Seneviratne S, Ko BS, Ito H et al. Diagnostic performance of noninvasive fractional flow reserve derived from coronary computed tomography angiography in suspected coronary artery disease: the NXT trial (Analysis of coronary blood flow using CT angiography: next steps). *J Am Coll Cardiol* 2014;**63**:1145–55.
  16. Cutlip DE, Windecker S, Mehran R, Boam A, Cohen DJ, van Es GA et al. Clinical end points in coronary stent trials: a case for standardized definitions. *Circulation* 2007;**115**:2344–51.
  17. Serruys PW, Garcia-Garcia HM, Onuma Y. From metallic cages to transient bioresorbable scaffolds: change in paradigm of coronary revascularization in the upcoming decade? *Eur Heart J* 2012;**33**:16–25b.
  18. Alberts B. *Molecular Biology of the Cell*. Vol. **xxxiv**, p1548, 4th ed. New York: Garland Science; 2002.
  19. Serruys PW, Onuma Y, Garcia-Garcia HM, Muramatsu T, van Geuns RJ, de Bruyne B et al. Dynamics of vessel wall changes following the implantation of the absorb everolimus-eluting bioresorbable vascular scaffold: a multi-imaging modality study at 6, 12, 24 and 36 months. *EuroIntervention* 2014;**9**:1271–84.
  20. Park HB, Heo R, o Hartaigh B, Cho I, Gransar H, Nakazato R et al. Atherosclerotic plaque characteristics by CT angiography identify coronary lesions that cause ischemia: a direct comparison to fractional flow reserve. *JACC Cardiovasc Imaging* 2015;**8**:1–10.
  21. Gaur S, Ovrehus KA, Dey D, Leipsic J, Botker HE, Jensen JM et al. Coronary plaque quantification and fractional flow reserve by coronary computed tomography angiography identify ischaemia-causing lesions. *Eur Heart J* 2016;**37**:1220–7.
  22. Ahmadi A, Stone GW, Leipsic J, Serruys PW, Shaw L, Hecht H et al. Association of coronary stenosis and plaque morphology with fractional flow reserve and outcomes. *JAMA Cardiol* 2016;**1**:350–7.
  23. Park SJ. *The Preventive Implantation of Bioresorbable Vascular Scaffold on Functionally Insignificant Stenosis With Vulnerable Plaque Characteristics*. <https://clinicaltrials.gov/ct2/show/NCT02316886> (16 June 2016, date last accessed).
  24. Erlinge D. *A Multicentre Prospective Natural History Study Using Multimodality Imaging in Patients With Acute Coronary Syndromes—PROSPECT II (Natural History Study), Combined With a Randomized, Controlled, Intervention Study—PROSPECT ABSORB (Randomized Trial)*. <https://clinicaltrials.gov/ct2/show/NCT02171065> (16 June 2016, date last accessed).
  25. Collet C, Sotomi Y, Cavalcante R, Asano T, Miyazaki Y, Tenekecioglu E et al. Accuracy of coronary computed tomography angiography for bioresorbable scaffold luminal investigation: a comparison with optical coherence tomography. *Int J Cardiovasc Imaging* 2016;**33**:431–9.